EASR

Engineering and Applied Science Research

https://www.tci-thaijo.org/index.php/easr/index

Published by the Faculty of Engineering, Khon Kaen University, Thailand

Optimisation of charge ratios for ball milling synthesis: agglomeration and refinement of coconut shells

Sefiu Adekunle Bello*[1, 2)], Johnson Olumuyiwa Agunsoye[2)], Jeleel Adekunle Adebisi[3)] and Suleiman Bolaji Hassan[2)]

[1)]Department of Metallurgical and Materials Engineering, College of Engineering and Technology, Kwara State University, Malete, Nigeria
[2)]Department of Metallurgical and Materials Engineering, Faculty of Engineering, University of Lagos, Nigeria
[3)]Department of Metallurgical and Materials Engineering, Faculty of Engineering, University of Ilorin, Nigeria

Received 20 January 2018
Accepted 27 April 2018

Abstract

Agglomeration is an attraction of fine particles for one another due to their high surface energy, leading to formation of particle colonies known as agglomerates. When a polymeric or metallic matrix is reinforced with particles, agglomerates usually create regions of discontinuity or weak particle adhesion within the matrix and degrade mechanical properties of the resulting composites. In ball-milling synthesis of nanoparticles, formation of agglomerates can be controlled through optimisation of milling parameters. In this study, coconut shell (lignocellulosic) nanoparticles were synthesised by varying the charge ratios from 2.5 to 40 at constant milling duration (70 hours), speed in terms of drum/vial rotation (194 revolution per minute) and ball sizes (5- 60 mm). Assessment of the effects of charge ratios (CRs) on the morphologies and particles sizes of uncarbonised coconut shell nanoparticles (UCSnp) was studied. The synthesised UCSnp were characterised using electron microscopy and X-ray diffractometry (XRD). The results showed various morphologies and orientations of UCSnp with changes in the CRs. Size determination using XRD and SEM revealed a reduction in particle size as the CR increased up to a value of 10. At higher CRs, further reduction in the average particle size was not observable. This could be linked to a balance between particle refinement and agglomeration at these higher CRs. Although particle agglomeration was apparent above CR values of 10, sizes of the UCSnp obtained above this CRs were much smaller than the initial size (37 μm) of the coconut shell precursor particles. This affirmed the ball milling synthesis as a particle refinement process, but not a coarsening/agglomeration process. The results obtained from statistical analyses show agreement with experimental results.

Keywords: Electron microscopy, Surface energy, X-ray study, Agglomerates, Synthesis

1. Introduction

Nanoparticles can be engineered when they are intentionally synthesised for a purpose or they may occur naturally. Synthesis of nanoparticles is usually accompanied by analysis of their properties to determine their sizes, morphology and other pertinent properties [1-7]. To determine nanoparticle sizes, various approaches can be used including theoretical calculation and image sizing. Theoretical approaches for nanoparticle size determination involves the use of formulas to aid experimental analyses. These include laser light diffraction, dynamic light scattering, sedimentation, Coulter counting, and differential mobility analyses. These techniques provide no information about nanoparticle morphology. Imaging tools such as scanning electron microscopy (SEM), atomic force microscopy (AFM) and transmission electron microscopy (TEM) can be used to reveal nanoparticle morphology in addition to particle size determination [2, 8-17].

Recent interest in using agricultural waste particles for reinforcing polymers to produce dispersion strengthening composites for engineering applications has paved the way for research into particle synthesis using various techniques [18-19]. Agricultural waste particle processing by ball-milling has been reported [20-25]. Although, synthesis of agricultural waste nanoparticles has been accomplished, particle agglomeration is a challenge [23, 26]. Particle agglomeration is a physical combination of particles that leads to integration or fusion of ultrafine particles during ball milling. It occurs when particles attain unstable high energy states because of their small sizes. Ultrafine particles seek energy minimization through fusion with one another and or with coarse particles to improve their stability. Consequently, formation of particle colonies, known as agglomerates, occurs. Particle agglomeration results in a relative particle coarsening and opposes particle refinement, which is the purpose of ball-milling. Alternatively, the presence of agglomerates among synthesised agricultural waste particles creates regions of discontinuity within a

*Corresponding author. Tel.: +234 8038 548418
Email address: belloshaafiu@gmail.com
doi: 10.14456/easr.2018.36

matrix when such particles are used as a reinforcing agent in matrix for composite development. Furthermore, diminished mechanical properties of the resulting composites due to particle agglomerates has been revealed in published literature reports [27-28]. Therefore, there is a need to optimize ball milling parameters such as charge ratios, milling duration, vial speed of rotation, size and nature of the milling balls to produce agricultural waste particles with few or no particle agglomerates. This study was focused on the use of coconut shells to increase their economic value via applications of the uncarbonised coconut shell nanoparticles (UCSnp) for composite development. A similar study may focus on other agricultural wastes that are abundant in various regions across the globe. Particle agglomeration has a link with particle sizes [23, 26]. Agglomeration begins when some particles have reached their finest state during ball milling, so that further milling causes size reduction of the coarse particles while the finest particles joins with one another and/or coarse particles [29]. However, to predict onset of particle agglomeration, knowledge of the minimum particle size (size of the finest particles) is very important. The charge ratio is defined as total mass of the milling balls divided by mass of the material to be refined. This is determined before the ball milling process has begun. It is done to estimate percentage of free space within the vial, which in turn determines collision impact of the milling balls with particles during ball milling. The effects of milling duration and vacuum carbonisation on the properties of coconut shell nanoparticles have been studied and reported [26, 29-30]. However, the influence of the charge ratio on the sizes and morphologies of coconut shell particles is a main focus of the present study. Moreover, threshold charge ratios, below which particle agglomeration has no significant influence on refinement of coconut shell particles via ball-milling, have been established experimentally and through nonlinear (Gaussian) curve fitting statistical analysis.

2. Materials and methods

The coconut shell nanoparticles used in this work were synthesised via a ball milling technique using 37 μm diameter coconut shell powders as a precursor in accordance with previous studies [26, 29]. Precursors were milled at various CRs, ranging from 2.5 to 40 using a SNH 510….680 tumbler ball mill, Model A 50….43 at the Federal Industrial Institute of Research Oshodi (FIIRO), Lagos, Nigeria. Other milling parameters such as milling duration (70 hours), speed (194 rpm), milling ball sizes (5-60 mm) and ball material (ceramic) were kept constant. The uncarbonised coconut shell nanoparticles were analysed and their sizes were determined using an ASPEX 3020 Scanning Electron Microscope/Energy Dispersive X-ray spectroscopy (SEM/EDX), Philips 301 Transmission Electron Microscope with Gwyddion software and an X-ray diffractometer (Model: PW 1830) at the University of Witwatersrand, Johannesburg, South Africa. The Scherrer equation was applied using X'Pert HighScore software. To predict agglomeration of UCSnp, the material with the smallest (minimum) sizes were considered at various charge ratios since these have the highest surface energies. Minimum crystal sizes obtained from XRD were used in the statistical analyses since the theoretical calculations involved in the XRD size determination used the Scherrer equation. This is unlike image size determination in the cases of SEM and TEM analyses. A mono-variate statistical regression analysis involving the charge ratio as a predictor variable at seven different levels with the minimum size as the dependent (response) variable was performed using OriginPro 8 software. Linear, multiple linear, polynomial and nonlinear regression analysis were used to establish a relationship between two variables. The regression coefficient of determination (R^2), probability value (Prob>F), significance level and Fisher's value were determined as well. A nonlinear Gaussian function was employed to relate the minimum crystal sizes with CRs because of its greater prediction level (higher R^2 value) and smaller p-value compared to other functions. The analysis was evaluated at $\alpha = 0.05$, indicating a 95 % confidence level. Analysis of variance (ANOVA) was performed to determine the significance of the regression analysis.

3. Results and discussion

3.1 Scanning electron micrographs of uncarbonised coconut shell nanoparticles

Figure 1 displays a SEM/EDX magnified image of bulk coconut shell, i.e., the precursor. The micrograph in Figure 1 presents the coconut shell as a solid body with surface discontinuities. The defects make the coconut shell appear to have many individual layers joined together in a singular geometric body. The surface discontinuities act as stress raisers, which aid in breakage of the coconut shell during crushing and pulverisation. EDX chemical analysis showed that the bulk coconut shell contained C, O, Na, Al, Si, P and K. This agrees with [26, 29]. Coconut shells, as an organic material, are expected to be rich in carbon. However, maximum elemental peak was attributed to O rather than C, resulting from moisture in the bulk coconut shells. Additionally, inorganic compounds in the coconut shells such as Na, Al, Si, P and K may also contribute to the maximum peak observed for O.

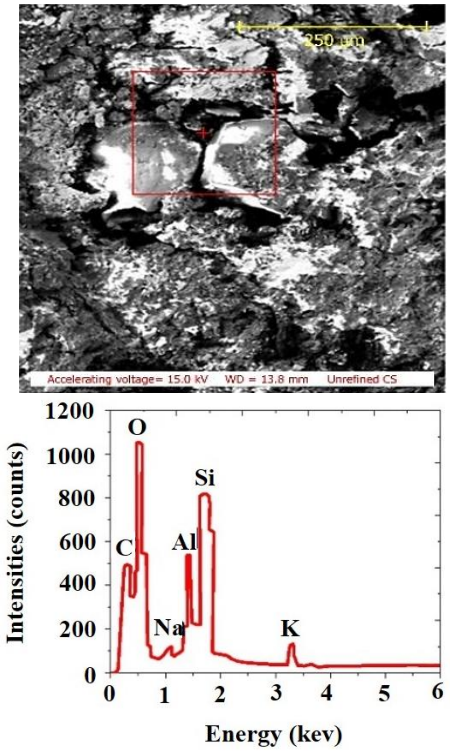


Figure 1 SEM/EDX showing the structural morphology of unrefined coconut shell and elemental composition of the coconut shell at the analysed area

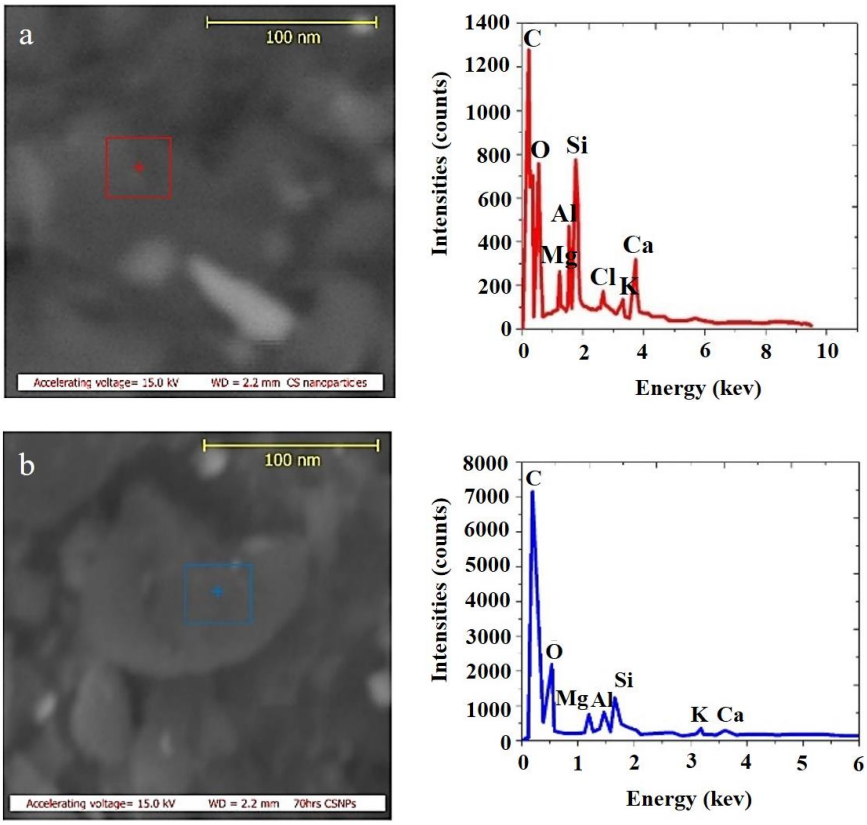


Figure 2 SEM/EDX of revealing morphology of coconut shell nanoparticles obtained at (a) 2.5 and (b) 5 charge ratios with their elemental composition at the analysed areas

The SEM images in Figures 2(a-b) reveal the morphology of the UCSnp obtained at 2.5 and 5 CRs and after 70 hours of milling. UCSnp appeared dull with various sizes and shapes. Individual UCSnp samples can easily be distinguished from one another. This is an indication that there was a gradual breakage of the precursor powders during the milling process with no sign of particle agglomeration. The UCSnp in Figure 2(b) appears smaller and less dull than its counterpart in Figure 2(a). The elemental composition of UCSnp in Figure 2 agrees with that of the bulk coconut shell in Figure 1. However, in terms of peak height, C had a greater peak than O. The C peak in Figure 2(a) had a height of about 1300 counts, 73 % higher than that of O peak, while in Figure 2(b), the C peak is 250 % taller than that of O. The increase in the C peak and fall of the O peak could be associated with drying of the UCSnp during the course of ball milling and associated temperature induced friction.

The SEM micrograph in Figure 3 shows the morphologies of UCSnp obtained with CR values of 10, 20 and 40. It was observed from Figure 3 that UCSnp exists in the form of fused solid bodies of various shapes, sizes and degrees of particle integration or agglomeration. The degree of particle integration increased as shown in Figure 3 as the CR value rose from 10 to 40. However, agglomerated particles in Figure 3(b-c) show many fine particles that were fused due to the increased surface area to volume ratio as the particle size reduction progressed during the course of ball milling. During this process, rotation of the mill vials caused a continual falling of grinding balls and particles during which the coconut shell particles collided with the milling balls and inner wall of the vial. This resulted in dissociation of the particles at point of tangential collisions between two balls or a ball and the inner surface of the drum/vial. These cause various fracture processess such as impact, tearing, compression and attrition, which are the driving forces for the breakage of the precursor particles, as shown in Figure 4. The extent of breakage increased as the CRs values rose from 2.5 to 40 (since the milling duration was constant) due to greater kinetic energy with which the balls impacted or struck the precursor particles. Comparison of Figure 2 with Figure 3 shows that there was a gradual breakage of the precursor particles, leading to formation of fine particles from coarse particles. As the breakage continued, surface energy of the newly formed fine particles increased, resulting in particles with a high energy state, especially above CR values of 10. This caused fusion or integration of fine particles to reestablish a minimum energy state, serving as a driving force for the formation of agglomerated particles, as shown in Figures 3(b-c). However, the degree of agglomeration increased with the CR value due to enhanced impacts by the milling balls. Such impacts subjected the particles to compressive forces which caused their fusion or integration. The enhancements in the impact were a function of increased kinetic energy due to incremental changes in the CR value. Brighter appearance of UCSnp can be linked to the fading of the brown colour of the coconut shell particles due to repeated plastic deformation induced breakage during the course of milling [26].

3.2 Transmission electron microscopic images of uncarbonised coconut shell nanoparticles

Figure 4 presents TEM images of UCSnp obtained at various CR values. The TEM images reveal each individual particle is approximately spherically shaped with varying degrees of particle agglomeration. By comparing the images

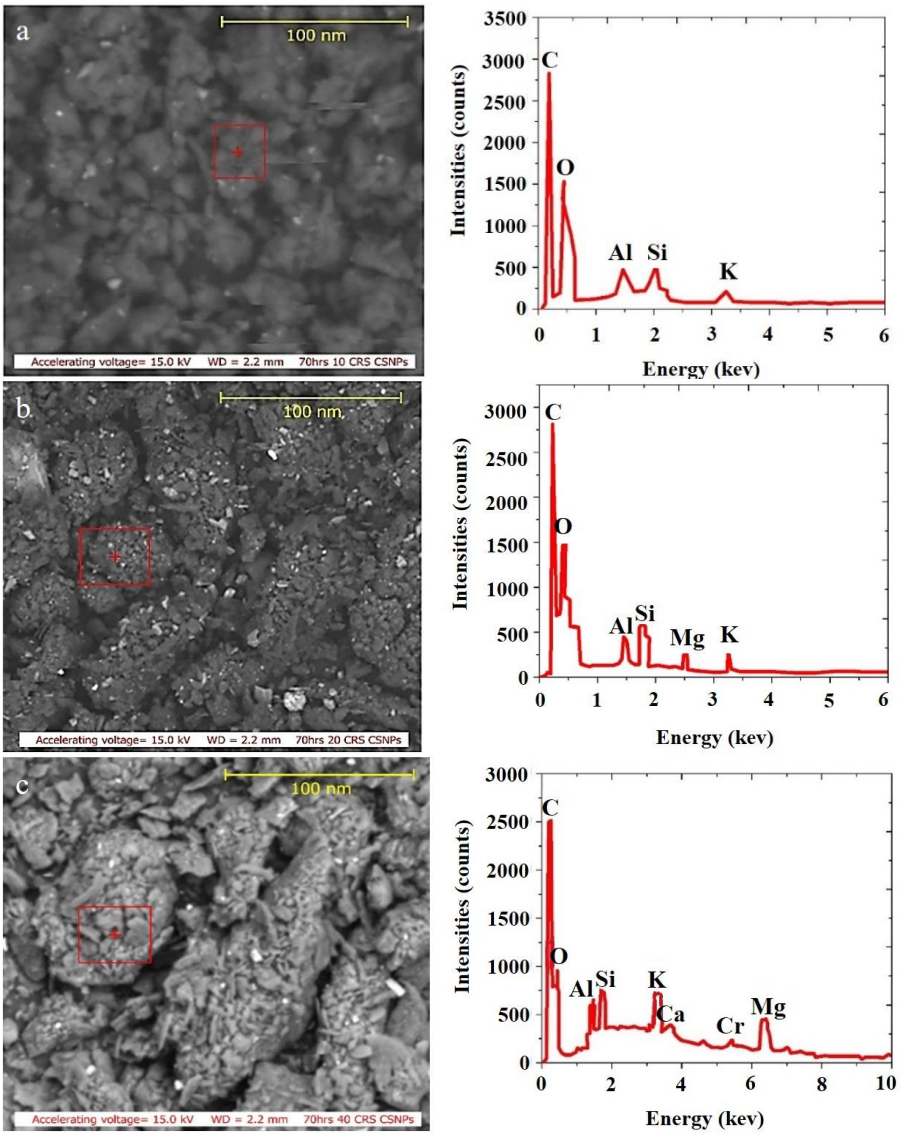


Figure 3 SEM/EDX showing various degrees of particle agglomeration within coconut shell nanoparticles obtained by milling for 70 hours at (a) 10, (b) 20 and (c) 40 charge ratios

from Figures 4(a-e), it can be observed that UCSnp appeared smaller as the CR value increased until it was above 10. Above this value the particles seemed larger than their counterparts at CR values of 10 or less. The larger sizes of the UCSnp above Cr values of 10 can be ascribed to their fineness and enhanced surface area, leading to interfacial particle adhesion. The ball impacts on the particles caused breakage of the particles at every collision between balls and UCSnp. This enhanced the Van der Waals' attraction and other intermolecular energies among the particles, leading to their fusion or clustering. A similar observation was made from the SEM micrographs in Figure 3.

3.3 X-ray diffraction of uncarbonised coconut shell nanoparticles

Figures 5-8 show the XRD profiles of UCSnp obtained at various CR values. The diffractogram in Figure 5 reveals an XRD profile of UCSnp obtained at a CR value of 2.5, showing C, $Al_2Si_2O_5(OH)_4$ and SiO_2 at various diffraction angles (2θ) ranging from 0 to 80˚. The same phases were observed in the XRD profiles of UCSnp obtained at a CR value of 5 in Figure 6, while the phases of UCSnp obtained at a CR value of 10 in Figure 7 were SiO_2 and C_2CaMgO_6 ($CaCO_3MgCO_3$) [26]. The consistency of SiO_2 in crystalline form in Figures 5-7 is an indication that coconut shells contain silicon compounds in addition to organic compounds such as cellulose and lignin. This is evidenced by the large hump in Figure 7 and published research results [31]. Formation of compounds such as $Al_2Si_2O_5(OH)_4$ and $CaCO_3MgCO_3$ can be linked to chemical interaction of various constituents of coconut shell particles during the ball milling process. This is in line with the published literature [32-35]. Figures 8-9 depict the XRD profiles of UCSnp obtained at CR values of 20 and 40. It was observed that SiO_2 was the only phase present. Absence of $Al_2Si_2O_5(OH)_4$ and $CaCO_3MgCO_3$ can be linked to agglomerated particles of SiO_2, which may have blocked the reflected X-rays from $Al_2Si_2O_5(OH)_4$ and $CaCO_3MgCO_3$ during the XRD analysis. A similar observation was made in the literature [33]. By matching (see Figure 10) the XRD profiles in Figures 5-9, it can be seen that the count score corresponding to the maximum peak of each diffractometry measurement

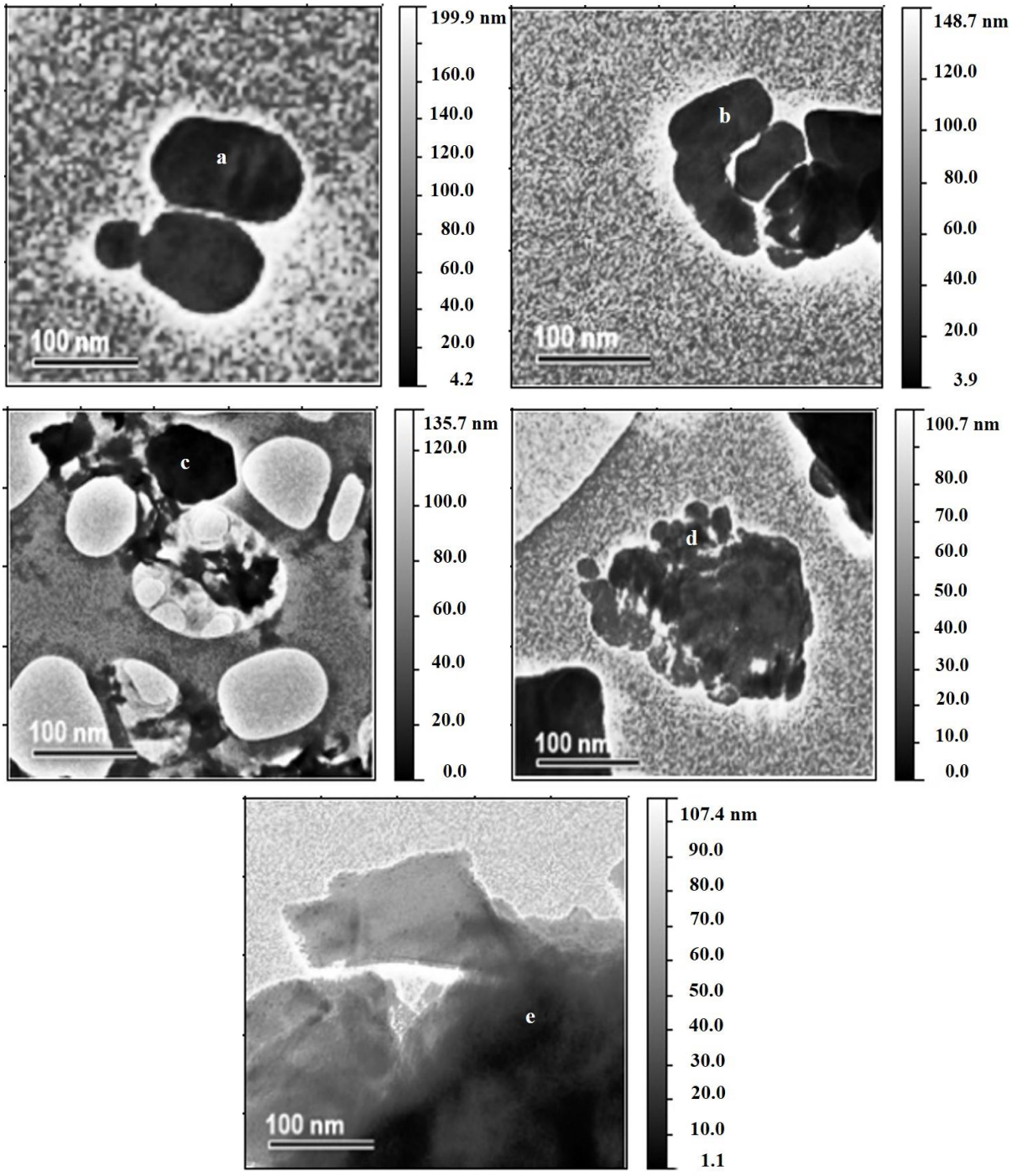


Figure 4 TEM images displaying degrees of particle agglomeration and size ranges of UCSnp obtained through milling for 70 hours at (a) 2.5, (b) 5 (c) 10 (d) 20 and (e) 40 charge ratios

increased incrementally with the CR value. Also, an incremental change in the peak widths reflects increased peak broadness as the CR increased to a value of 10 (see Figures 5-7). Above a CR value of 10, further peak broadness was not observed (see Figures 8-9). The peak broadness up to a CR value of 10 indicated continual breakage of coconut shell particles, resulting in a decrease in their sizes. However, above this CR value , fine particles with high surface energy adhered to one another to form agglomerated particles with reduced surface energy. This is supported by the SEM micrographs and TEM images in Figures 2-5. In previous work, similar agglomeration was observed with uncarbonised and carbonised coconut shell nanoparticles after 46 and 16 hours of ball milling, respectively, at a CR value of 10 [26, 30, 36]. Since the UCSnp and CCSnp are synthesised to serve as nanoparticles for polymer and metal reinforcement [19, 37], optimisation of ball milling parameters is important to obtain nanoparticles with little or no agglomeration. Nanoparticle agglomeration is undesirable in a composite matrix. Agglomerates are discontinuous domains within a matrix and diminish the mechanical properties of the composites [38].

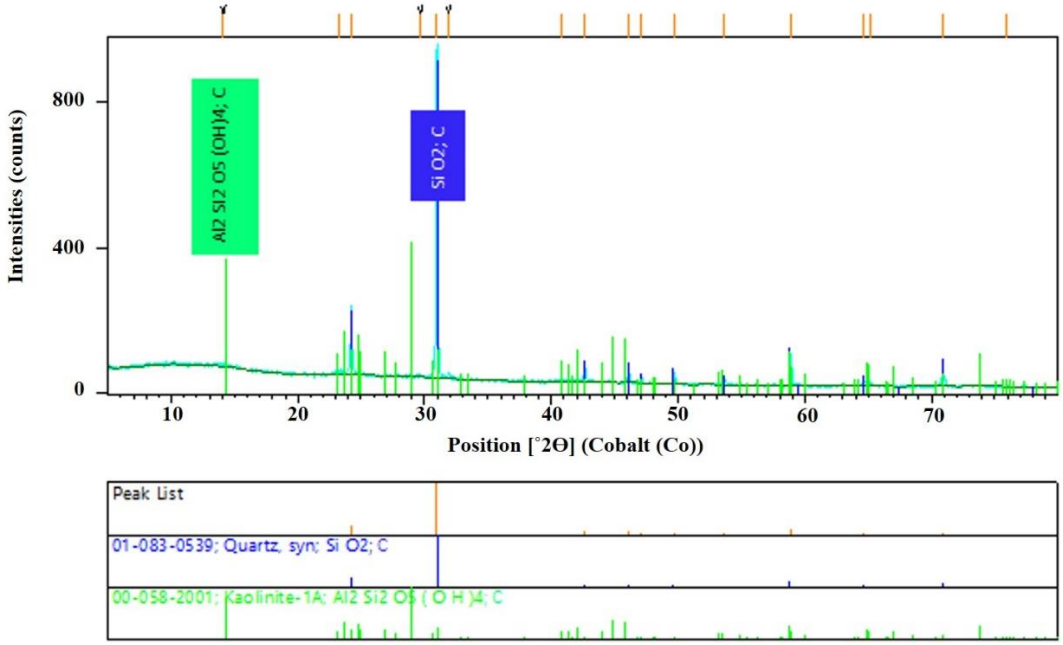


Figure 5 X-ray diffractometric properties of uncarbonised coconut shell nanoparticles obtained via milling for 70 hours at a charge ratio of 2.5, showing various phases at different diffraction angles, 2θ

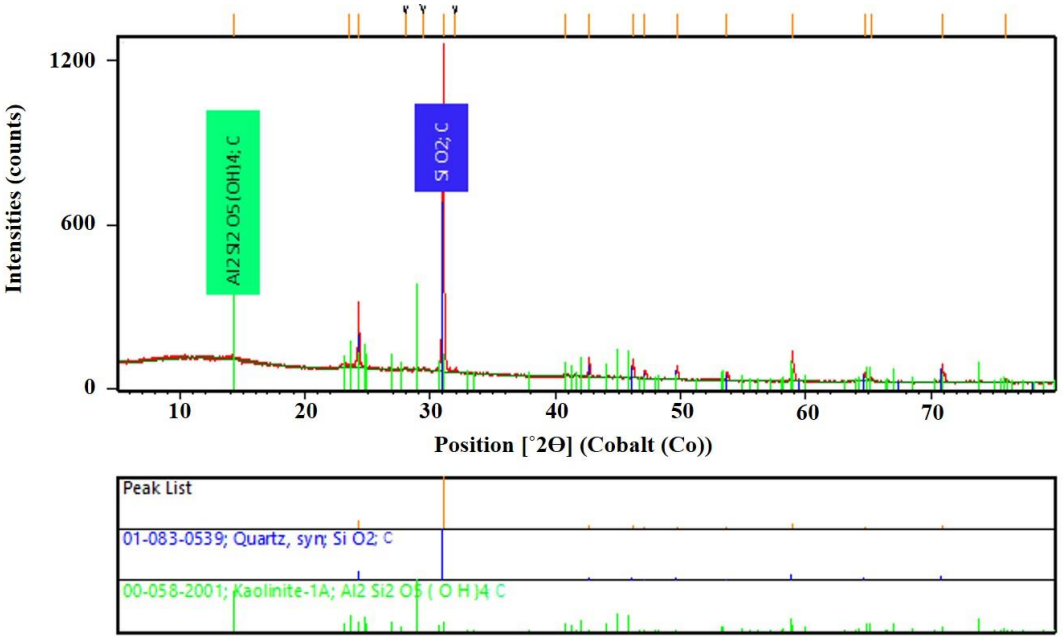


Figure 6 X-ray diffractometric properties of uncarbonised coconut shell nanoparticles obtained by milling for 70 hours at a charge ratio of 5 showing various phases at different diffraction angles, 2θ

3.4 Particles sizes and charge ratios

Figures 4(a-e) presents the sizes of UCSnp determined from TEM images using Gwyddion software. UCSnp obtained at a CR of 2.5 after 70 hours of ball milling had approximate diameters of 4 to 200 nm as revealed in Figure 4(a). Figure 4(b) shows that sizes of UCSnp nanoparticles produced at a CR of 5 after 70 hours of ball milling varied from 4 to 149 nm. In Figure 4(c), the sizes of UCSnp nanoparticles produced at a CR of 10 with 70 hours of ball milling varied between 0 and 136 nm. The sizes of UCSnp produced at a CR of 20 were between 0 and 101 nm, while the minimum and maximum sizes of UCSnp produced with a CR value of 40 were 1.1 and 107.4 nm, respectively (see Figures 4(d-e)). The minimum sizes of UCSnp obtained from XRD at CR values of 2.5, 5, 10, 20 and 40 were 11.8, 10.95, 2.95, 7.97 and 13.43 nm, respectively. The respective maximum sizes were 133.07, 113.11, 153.58, 97.28 and 266.43 nm. Average corresponding sizes of UCSnp obtained from TEM, SEM and XRD are shown in Figure 11. To ensure the accuracy of our results, these experiments were done in triplicate and the results averaged. Each bar in Figure 11 represents the mean sizes (obtained from SEM, TEM and XRD) of three UCSnp samples and the error bars indicate the standard deviations of these measurements (SEM, TEM and XRD). All XRD peaks, attributed to the

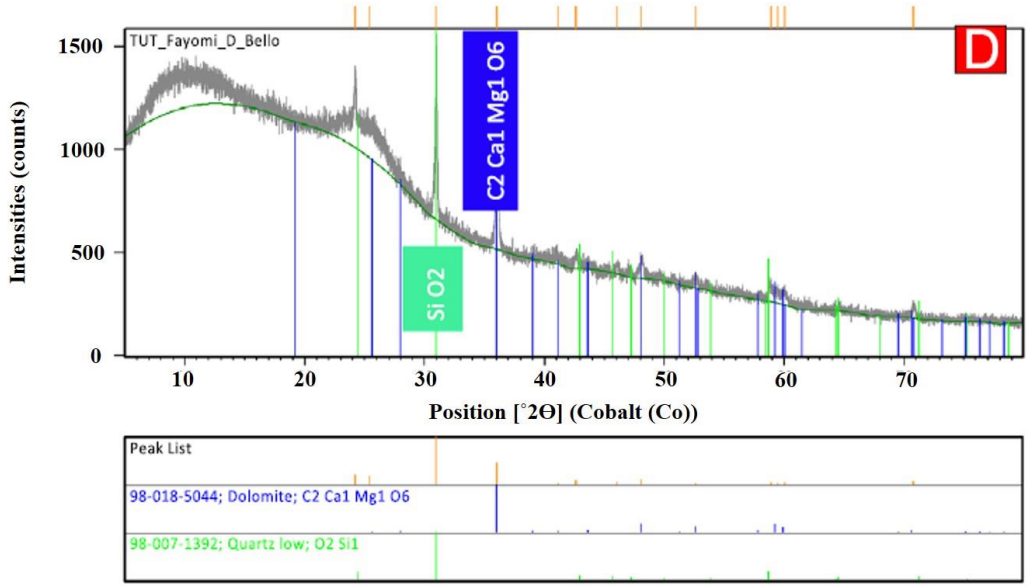


Figure 7 X-ray diffractometric properties of uncarbonised coconut shell nanoparticles obtained by ball milling for 70 hours at a CR value of 10 showing phases at different diffraction angles, 2θ

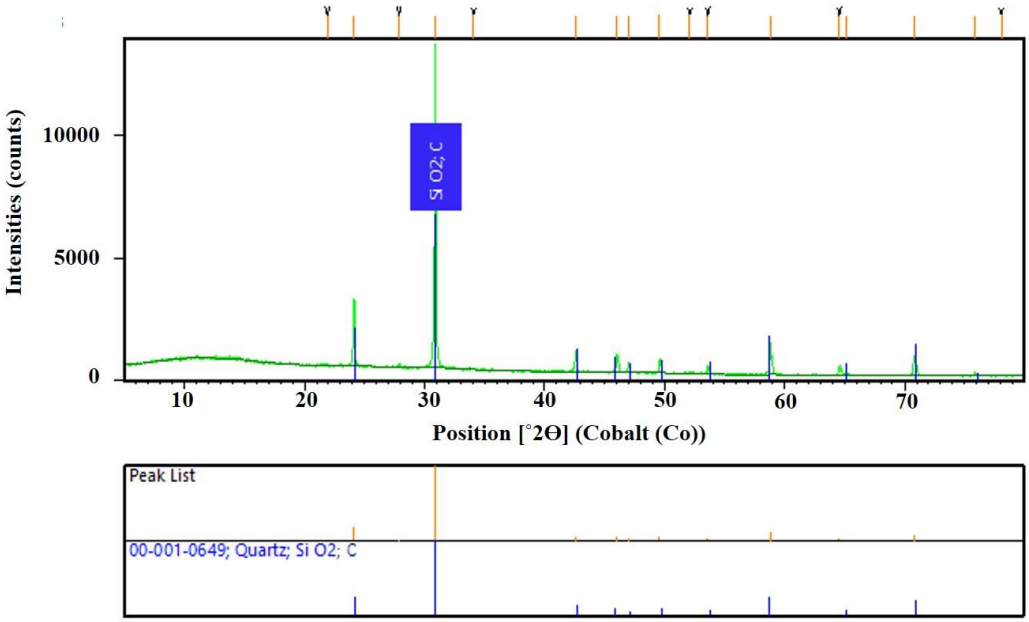


Figure 8 X-ray diffractometric properties of uncarbonised coconut shell nanoparticles obtained via ball-milling for 70 hours at a CR value of 20 showing phases at different diffraction angles, 2θ

phases in Figures 5-9, were used in determining the sizes of UCSnp at 2.5, 5 10, 20 and 40 CRs, respectively, using the Scherrer equation (Section 2). Generally, the observation from Figure 11 was that the average size decreased with increasing CR values. This observation is similar to reports of particle refinement with increased duration of ball milling [24-25, 39]. The decrease in the average particle size was very apparent up to a CR value of 10. Above this, further reduction in the average particle size was not observable in SEM images and XRD, while TEM revealed a gradual decrease in the sizes, though the decrease was less than that observed at CR values of 10 and less. At CR values above 10, there is a balance between further reduction in particle size and particle agglomeration. As the ball milling progressed, uneven distribution of the ball impacts on the particles caused differences in particle breakage. This resulted in production of both fine and relatively coarse particles at any instant in the ball mill. An increase in the CR value enhanced the magnitude of the ball impacts on the particles with consequent particle refinement and agglomeration. Particle refinement with increased milling duration has been reported in literature [40-41]. Similarly, differences in TEM and XRD sizes of Nano-crystalline 6061 Al powder produced by cryogenic milling has been revealed [39]. Also, size differences of Al (1xxx) nanoparticles obtained from TEM, SEM and XRD were attributed to discrepancies in equipment operation [42-43]. In the present study, differences in crystalline and particles sizes likely occurred since only crystalline phases (XRD peaks) were used in the crystal size determination, while crystalline and

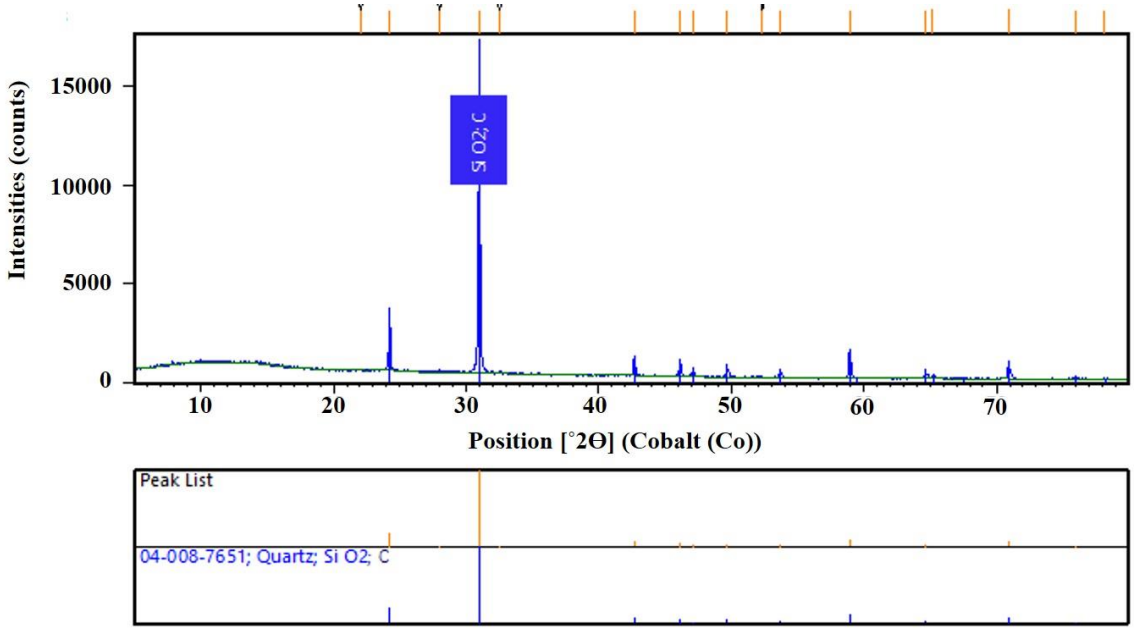


Figure 9 X-ray diffractometric properties of uncarbonised coconut shell nanoparticles obtained by milling for 70 hours at a CR value of 20 showing phases at different diffraction angles, 2θ

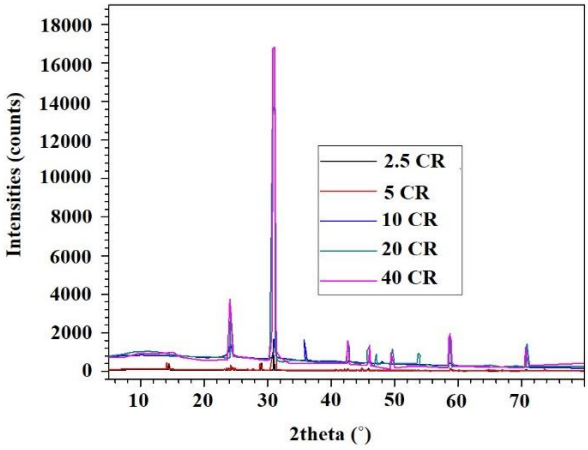


Figure 10 Superimposed XRD profiles of UCSnp revealing peaks with different intensities and broadness

amorphous phases were involved in image sizing analyses by SEM and TEM aided by software. Therefore, these findings are in agreement with literature observations [23, 39, 42].

A balance between particle refinement and agglomeration is required to attain minimum sizes of lignocellulosic particles. At its minimum size, UCSnp are characterised by high surface energy. They are thermodynamically unstable. Agglomeration of fine particles minimises their energy and restores their stability. The scatter plot in Figure 12 present the variation of the minimum particle size of UCSnp obtained from XRD at various CRs. It was observed that UCSnp attained a minimum size at a CR value of 10. This implied that, in milling precursor particles for 70 hours, the finest particles have high tendency to form stable clusters at CR values above 10. Moreover, to establish the exact CR above which particle agglomeration counters particle refinement, minimum particle sizes and charge ratios were analysed using a spline curve and nonlinear regression with a Gaussian function as shown in Figure 12. Minimum size (Ms) of the UCSnp was used as the dependent variable (response) while the CRs were predictors. A formula for predicting the Ms obtained from nonlinear (Gaussian) regression analysis is expressed in Equation 1, while Table 1 reveals values and standard errors of each parameter used in Equation 1. Ms (see Table 2) at any CR of interest, within and outside the scope of the analysis can be estimated through substitution of the values of y_o, A, w, x_c in Table 1 and the CR in Equation 1.

$$M_s = y_o + \left(\frac{A}{w\sqrt{\frac{\pi}{2}}}\right) e^{-2\left(\frac{CR-x_c}{w}\right)^2} \quad (1)$$

The discrepancies between the actual and the predicted values of Ms are presented as residuals in the last column of Table 2. The residuals account for variance of the adjusted R-square from unity (100%). The coefficient of determination (R^2) was 0.91597, which accounted for 91.6 % of the observed data.

Table 1 Values and standard errors of parameters characterising the model function

	y_o		x_c		W		A		Sigma	FWHM	Height	Statistics	
	Value	Error	Value	Error	Value	Error	Value	Error				Reduced Chi-Square	Adj. R-Square
B	12.98985	1.09	13.48657	0.579	9.4209	1.76	-154.79829	27.94	4.71045	11.09227	-13.11033	1.37486	0.91597

y_o- is the minimum particle size at the onset of milling, x_c- is the threshold charge ratio, W- is the full width half maximum, A-is the amplitude, π is a constant (3.142)

Table 2 Confirmation and validation of experiments

Charge Ratios	Ms (nm)		
	Actual	Predicted	Residual
2.5	11.19	12.12621	-0.93621
5	10.95	10.40302	0.54698
10	2.95	3.02097	-0.07097
20	7.97	7.94995	0.02005
40	13.43	12.98985	0.44015

Table 3 Analysis of variance (ANOVA) for UCSnp

Analysis Elements	DF	Sum of Squares	Mean Square	F Value	Prob>F
Regression	4	496.33204	124.08301	90.2517	0.04719
Residual	1	1.37486	1.37486		
Corrected total	4	65.44288			

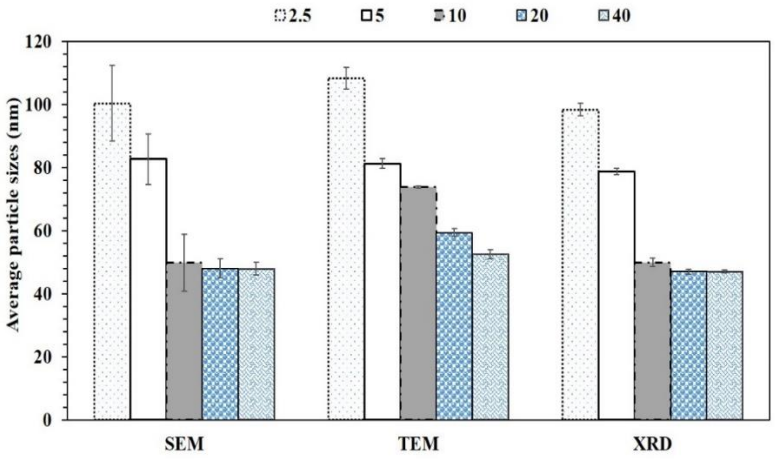


Figure 11 Histogram presenting average sizes of uncarbonised coconut shell nanoparticles obtained by ball milling for 70 hours at various charge ratios determined from different particle size analyses (XRD, SEM and TEM)

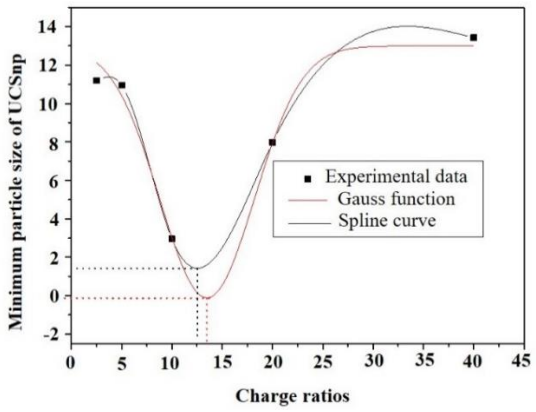


Figure 12 Variation of UCSnp minimum sizes with charge ratios

The equation/function developed demonstrates a good prediction of the experimental data. This agrees with observations in the literature [44-45]. Table 3 shows that values of Prob>F and the F-value are 0.04719 and 90.2517, respectively. This implies that the Gaussian regression analysis is effective in establishing a relationship between Ms and CRs with a high F-value (90.2517) affirming that there is a very low level of noise in the calculations with four degrees of freedom in developing the function given by Equation 1.

Moreover, the experimental data showed the attainment of the finest particles at a CR value of 10, while the results obtained from regression analysis revealed a threshold CR of 13.49±0.6. The implication of this is that at the threshold CR (13.49±0.6), some of UCSnp are so fine that further increase in CRs promotes their agglomeration. Then, the effect of particle agglomeration counters particle size reduction such

that further reduction in the size of milled UCSnp is diminished and opposite effect is achieved. There is good agreement between the regression analysis and experimental results. Therefore, it is inferred, based on the results of the regression analysis, that the maximum threshold CR for obtaining UCSnp through ball milling is 13.49±0.6. Above this CR value, prolong ball milling of UCSmp (37 μm) leads to greater particle agglomeration. Below 13.49±0.6 CRs, particle refinement is very high. However, above a CR value of 13.49±0.6, particle agglomeration dominates particle refinement leading to little further reduction in particle sizes, as supported by the TEM data in Figure 4 as well as SEM and XRD.

4. Conclusions

The effects of charge ratio on agglomeration and refinement of coconut shells were studied. The sizes of uncarbonised coconut shell were determined using SEM, TEM and XRD. Statistical analysis was done to establish the relationship between sizes of the finest coconut shell particles and charge ratios as a tool to predict formation of stable particle agglomerates during ball milling. Broadening of the XRD peaks as the CR increased is an indication of a decrease in particle size. XRD, SEM and TEM results revealed a decrease in the UCSnp average sizes with an incremental increase in the CR. Experimental data, spline curve fitting and Gaussian models revealed that a balance is reached between particle refinement and agglomeration at 10, 12.5 and 14.261 CRs such that ball-milling of 37 μm diameter coconut shell powders for 70 hours above the specified CRs resulted in formation of stable particle agglomerates that retarded further reduction in the average sizes of UCSnp. Both spline curve fitting and Gaussian regression show fair agreement with the experimental data.

5. Acknowledgements

The authors wish to express their gratitude to the staff members of the Ceramics Department of the Federal Industrial Institute of Research Oshodi, Nigeria for their support. Also, this research project was sponsored by a TETFUND-IBR grant (KWASUNGR/CSP/251116 /VOL3/TETF/0037) accessed through the Centre for Sponsored Projects, Kwara State University, Malete, Nigeria.

6. References

[1] Moreno R, Ferrari B. Nanoparticles dispersion and the effect of related parameters in the EPD kinetics. In: Dickerson J, Boccaccini A, editors. Electrophoretic Deposition of Nanomaterials. Nanostructure Science and Technology. New York: Springer; 2012. p. 73-128.

[2] Lowndes DH. Nanoscale science, engineering and technology research directions. USA: Oak Ridge National Laboratory; 1999.

[3] Pokropivny V, Lohmus R, Hussainova I, Pokropivny A, Vlassov S. Introduction to nanomaterials and nanotechnology. Estonia: Tartu University Press; 2007.

[4] Aïcha H, Marco C, Duncan A. Transmission electron microscopy and diffraction. Switzerland: Centre interdisciplinaire de Microscopie Electronique (CIME), Photovoltaics and Thin-Film Electronics Laboratory (PV-lab); [date unknown].

[5] FEI COMPANY. All you wanted to know about Electron Microscopy. USA: FEI COMPANY; [date unknown].

[6] Mogilatenko A, Kirmse H. Transmission electron microscopy in materials science. Berlin: Humboldt-Universität zu Berlin; [date unknown].

[7] Zinin P. GG 711: Advanced techniques in geophysics and materials science HIGP. USA: University of Hawaii; [date unknown].

[8] Echin P. Handbook of sample preparation for scanning electron microscopy and x-ray microanalysis. USA: Springer; 2009.

[9] University of Babylon. Chapter 3: Transmission electron Microscopy. Iraq: University of Babylon; [date unknown]. p. 21-42.

[10] EA Group. Aberration corrected scanning transmission electron microscopy (AC-STEM) services. San Diego: Evans Analytical Group; 2014.

[11] Ma H, Shieh KJ, Qiao TX. Study of transmission electron microscopy (TEM) and scanning electron microscopy (SEM). Nat Sci. 2006;4(3):14-22.

[12] Voutou B, Stefanaki E. Electron microscopy: The Basics. Physics of Advanced Materials Winter School. 2008:1-11.

[13] Wang C, Liu Y. EMA 6518: Transmission Electron Microscopy. USA: Advanced Materials Engineering Research Institute (AMERI). [date unknown].

[14] Wang D. Transmission Electron Microscopy. USA: Swagelok Centre for Surface Analysis of Materials, Case Western Reserve University; 2016.

[15] Wang ZL. Transmission electron microscopy of Shape-controlled nanocrystals and their assemblies. J Phys Chem B. 2000;104(6):1153-75.

[16] Wang ZL. New development in transmission electron microscopy for nanotechnology. Adv Mater. 2003;15(18):1498-514.

[17] Zheng JG. What can electrons do?. USA: EPIC/NUANCE Center, Northwestern University; 2006.

[18] Bello SA. Development and characterisation of epoxy-aluminium-coconut shell particulate hybrid nanocomposites for automobile applications. Nigeria: Department of Metallurgical and Materials Engineering, University of Lagos; 2017.

[19] Bello SA, Agunsoye JO, Hassan SB, Zebase Kana MG, Raheem IA. Epoxy resin based composites, mechanical and tribological properties: a review. Tribology in Industry. 2015;37(4):500-24.

[20] Sarki J, Hassan SB, Aigbodion VS, Oghenevweta JE. Potential of using coconut shell particle fillers in eco-composite materials. J Alloy Comp. 2011;509(5): 2381-5.

[21] Knieke C, Steinborn C, Romeis S, Peukert W, Breitung-Faes S, Kwade A. Nanoparticle production with stirred-media mills: opportunities and limits. Chem Eng Tech. 2010;33(9):1401-11.

[22] Prasad Yadav T, Manohar Yadav R, Pratap Singh D. Mechanical milling: a top down approach for the synthesis of nanomaterials and nanocomposites. Nanoscience and Nanotechnology. 2012;2(3):22-48.

[23] Sommer M, Stenger F, Peukert W, Wagner NJ. Agglomeration and breakage of nanoparticles in stirred media mills—a comparison of different methods and models. Chem Eng Sci. 2006;61(1):135-48.

[24] Breitung-Faes S, Kwade A. Nano particle production in high-power-density mills. Chem Eng Res Des. 2008; 86(4):390-4.

[25] Essl F, Bruhn J, Janssen R, Claussen N. Wet milling of Al-containing powder mixtures as precursor materials for reaction bonding of alumina (RBAO) and reaction sintering of aluminium-aluminide alloys (3A). Mater Chem Phys. 1999; 61(1):69-77.

[26] Bello SA, Agunsoye JO, Hassan SB. Synthesis of coconut shell nanoparticles via a top down approach: assessment of milling duration on the particle sizes and morphologies of coconut shell nanoparticles. Mater Lett. 2015;159:514-9.

[27] Agunsoye JO, Aigbodion VS. *Bagasse Filled Recycled Polyethylene Bio-composites: Morphological and Mechanical Properties Study.* Results in Physics. 2013;3:187-94.

[28] Atuanya CU, Edokpia RO, Aigbodion VS. The physio-mechanical properties of recycled low density polyethylene (RLDPE)/bean pod ash particulate composites. Results in Physics. 2014;4:88-95.

[29] Bello SA, Hassan SB, Agunsoye JO, Kana MGZ, Raheem IA. Synthesis of uncarbonised coconut shell nanoparticles: characterisation and particle size determination. Tribology in Industry. 2015;37:257-63.

[30] Bello SA, Agunsoye JO, Adebisi JA, Kolawole FO, Suleiman BH. Physical properties of coconut shell nanoparticles. Kathmandu University Journal of Science, Engineering and Technology. 2016; 12(1):63-79.

[31] Agunsoye JO, Talabi SI, Bello SA, Awe IO. The effects of cocos nucifera (coconut shell) on the mechanical and tribological properties of recycled waste aluminium can composites. Tribology in Industry. 2014;36(2):155-62.

[32] Chauruka SR, Hassanpour A, Brydson R, Roberts KJ, Ghadiri M, Stitt H. Effect of mill type on the size reduction and phase transformation of gamma alumina. Chem Eng Sci. 2015;134:774-83.

[33] Liu T, Shen H, Wang C, Chou W. Structure evolution of Y2O3 nanoparticle/Fe composite during mechanical milling and annealing. Progr Nat Sci. 2013; 23(4):434-9.

[34] Qu Y, Luo H, Li H, Xu J. Comparison on structural modification of industrial lignin by wet ball milling and ionic liquid pretreatment. Biotechnology Reports. 2015;6:1-7.

[35] Yang F, Yan G, Wang QY, Xiong XM, Li SQ, Liu GQ, et al. The effect of high-energy ball milling on the microstructure and properties of ti-doped mgb2 bulks and wires. Physics Procedia. 2015;65:157-60.

[36] Hassan SB, Agunsoye JO, Bello SA. Characterization of coconut shell nanoparticles using electron microscopes. Proceedings of 10th UNILAG Annual Research Conference and Fair; 2015 Nov 24-26; Lagos , Nigeria. Lagos: University of lagos; 2015. p. 221-5.

[37] Agunsoye JO, Bello SA, Bello L, Idehenre MM. Assessment of mechanical and wear properties of epoxy based hybrid composites. Adv Produc Engineer Manag. 2016;11(1):5-14.

[38] Asuke F, Aigbodion VS, Abdulwahab M, Fayomi OSI, Popoola API, Nwoyi CI, et al. Effects of bone particle on the properties and microstructure of polypropylene/bone ash particulate composites. Results in Physics. 2012;2:135-41.

[39] Hanna W, Maung K, El-Danaf EA, Almajid AA, Soliman MS, Mohamed FA. Nanocrystalline 6061 Al powder fabricated by cryogenic milling and consolidated via high frequency induction heat sintering. Advances in Materials Science and Engineering. 2014;2014:1-9.

[40] Varol T, Canakci A, Yalcin ED. Fabrication of nanoSiC-reinforced Al2024 matrix composites by a novel production method. Arab J Sci Eng. 2016;42(5):1751-64.

[41] Wolff MFH, Antonyuk S, Heinrich S, Schneider GA. Attritor-milling of poly(amide imide) suspensions. Particuology. 2014;17:92-6.

[42] Bello SA, Agunsoye JO, Adebisi JA, Anyanwu JE, Bamigbaiye AA, Hassan SB. Potential of Carbonised Coconut Shell as a Ball-Milling Interface for Synthesis of Aluminium (1xxx) Nanoparticles. ANNALS of Faculty Engineering Hunedoara–International Journal of Engineering. 2017;15:149-57.

[43] Bello SA, Agunsoye JO, Adebisi JA, Kolawole FO, Raji NK, Hassan SB. Quasi crystal al (1xxx)/carbonised coconut shell nanoparticles: synthesis and characterisation. MRS Advances. 2018:1-13.

[44] Agunsoye JO, Bello SA, Adetola LO. Experimental investigation and theoretical prediction on tensile properties of particulate reinforced polymeric composites. Journal of King Saud University - Engineering Sciences. In press 2017.

[45] Atuanya CU, Aigbodion VS, Nwigbo SC. Experimental study of the thermal and wear properties of recycled polyethylene/breadfruit seed hull ash particulate composites. Mater Des. 2014;53:65-73.